

Article

Development of a Wide-Range Non-Dispersive Infrared Analyzer for the Continuous Measurement of CO₂ in Indoor Environments

Trieu-Vuong Dinh ¹, Joo-Yeon Lee ¹, Ji-Won Ahn ² and Jo-Chun Kim ^{1,*}¹ Department of Civil and Environmental Engineering, Konkuk University, 120 Neungdong-ro, Gwangjin-Gu, Seoul 05029, Korea; dinhtrieuvuong@gmail.com (T.-V.D.); joooyeon07@gmail.com (J.-Y.L.)² International Climate and Environmental Research Center, Konkuk University, 120 Neungdong-ro, Gwangjin-Gu, Seoul 05029, Korea; jwahn81@konkuk.ac.kr

* Correspondence: jckim@konkuk.ac.kr; Tel.: +822-450-4009; Fax: +822-3437-8654

Received: 16 August 2020; Accepted: 21 September 2020; Published: 23 September 2020



Abstract: Carbon dioxide (CO₂) is an indicator of indoor air quality. Ventilation based on the use of a CO₂ indicator helps to prevent people from acquiring many diseases, especially respiratory viral infections. Therefore, the monitoring of CO₂ is a pivotal issue in the control of indoor air quality. A nondispersive infrared (NDIR) analyzer with a wide range of measurements (i.e., ppmv to percentage levels) was developed for measuring carbon dioxide (CO₂) in an indoor environment. The effects of optical pathlength and interfering gases were investigated. The pathlengths of the analyzer were varied at 4.8, 8, 10.4 and 16 m, and the interference gases were CO; NO₂; SO₂; H₂O; BTEX (i.e., benzene, toluene, ethylbenzene and m-/p-xylene) and formaldehyde. The lower detection limit, selectivity and sensitivity were determined to evaluate the performance of the analyzer. It was found that different pathlengths should be used to produce linear calibration curves for CO₂ from ppmv to percentage levels. As a result, a wide-range NDIR analyzer, coupled with flexible pathlengths from 4.8 to 10.4 m, was developed. In terms of interference, only H₂O should be taken into account due to its high concentration in indoor air. CO should be considered in some special locations at the ppmv level. The measurement errors for ppmv and the percentage levels were 0.4 and 0.9%, respectively.

Keywords: carbon dioxide; indoor air; NDIR; pathlength; interference

1. Introduction

Besides being a greenhouse gas in the atmosphere, carbon dioxide (CO₂) also plays an important role in indoor environments [1–7]. CO₂ is an indoor air quality indicator [8–18]. CO₂ is the principal product of the combustion of fossil fuels and biomass. Therefore, it can function as a fire alarm indicator for the indoor environment in which it is present at high concentrations [1–3,5]. It is well-known that CO₂ is a metabolic gas generated from the human respiratory process [7]. A high concentration of CO₂ in an indoor environment influences mental activities, with effects such as increased errors when reading texts (at 3000 ppm of CO₂), decreased cognitive and behavioral responses (at 1000~2500 ppm of CO₂), an increase in end-tidal CO₂ levels and reduced heart rate (at 1000~3000 ppm of CO₂), difficulty in breathing (at 0.5%~3% of CO₂) and unconsciousness (at 7~10% of CO₂) [4,6,7]. Moreover, the concentration of CO₂ in the indoor environment also reflects the quality of the ventilation system of a building [6]. Recently, the pandemic caused by the SARS-CoV-2 virus has caused a serious crisis throughout the world. Ventilation has been reported as one of the primary methods used to reduce the rate of infection of the virus in indoor environments, which may result in a decline in the overall infection rate due to the fact that people spend most of the time in buildings [19]. Du et al. (2019) reported that a tuberculosis outbreak could be controlled when the ventilation rate of a building was

improved to a level with $\text{CO}_2 < 1000 \text{ ppmv}$ [8]. The American Society of Heating, Refrigerating, and Air Conditioning Engineers recommends that indoor CO_2 concentrations should not exceed the outdoor CO_2 concentration by more than 650 ppmv [13]. Accordingly, CO_2 monitoring is a pivotal issue in the indoor environment.

Until recently, CO_2 has been continuously measured by Fourier-transform infrared (FTIR) spectroscopy, cavity ring-down spectroscopy (CRDS), off-axis integrated cavity output spectroscopy (OA-ICOS) and nondispersive infrared (NDIR) spectroscopy [20]. A FTIR analyzer consists generally of a glow bar infrared (IR) source, a detector and an interferometer. The FTIR analyzer determines the infrared spectral information simultaneously, as opposed to a few frequencies at a time. Instead of selecting a specific wavelength or region within the entire infrared region concerned, the FTIR light source uses all the frequencies in the IR region of concern [21]. A CRDS analyzer includes a laser source, highly reflective mirrors and a detector. It measures the changes in the decay rate of light. The time of light decay provides an exact, noninvasive and rapid means of detecting contaminants in gases [21,22]. An OA-ICOS analyzer also comprises high-reflectivity mirrors, as in the CRDS method. Unlike CRDS, OA-ICOS does not require sophisticated optical and electronic components for the optical mode matching and coupling of the single-frequency laser to the optical cavity modes [23]. Among these techniques, NDIR technology has been widely used to determine CO_2 concentrations [24–30]. As an application of infrared spectroscopy, NDIR technology has been used to detect air pollutants that can absorb the infrared spectrum [31]. A typical NDIR analyzer consists of a light source, a light chopper, a gas chamber and a detector, coupled with a band-pass filter [32]. Various infrared (IR) light sources with different materials, such as a laser, Globar, Nernst glower and nichrome wire, can be used [31]. The light chopper is a rotating solid disk with several apertures that periodically interrupts the light beam [32,33]. The gas chamber is an empty box where sample gases contact with an IR beam. An IR detector is a device converting the temperature into an electrical signal. Thermal and quantum types are the two main ones of IR detectors [34]. Each target gas absorbs IR light at a specific wavelength (e.g., CO_2 at $4.26 \mu\text{m}$, CO at $4.6 \mu\text{m}$, NO at $5.3 \mu\text{m}$, NO_2 at $6.23 \mu\text{m}$, etc.). By using different IR band-pass filters (BPF), many gases can be analyzed at the same time with one IR source and detector [32]. A BPF is a nondispersive element that allows IR radiation at a specific wavelength [31]. The BPF comprises multilayered thin films that are attached on a substrate such as glass [32]. In a comparison with other spectroscopic techniques, NDIR has low energy consumption, because IR sources with wavelengths in the range of $1\text{--}15 \mu\text{m}$ can operate at a lower temperature than other sources [35].

Studies on CO_2 sensors and analyzers for indoor air have not been well-documented. There were only several studies on wide-range measurements of CO_2 with conditions similar to the indoor environment [29,30]. Vincent and Gardner (2016) developed a CO_2 sensor for breath analysis at ppm levels. The sensor was coupled with a micro-electromechanical system (MEMS)-based IR source. Since a MEMS-based IR source could electronically pulse to produce interruption IR beams, a beam chopper was unnecessary. This helped to reduce the size of the sensor. The gas chamber was a 10-mm aluminum tube. A thermopile detector coupled with a $4.26\text{-}\mu\text{m}$ BPF was used to detect CO_2 . The detectivity of the detector was $1.4 \times 10^8 \text{ cmHz}^{1/2}/\text{W}$. The measurement range of the sensor was from 50 ppm to 2.5%. It was reported that the accuracy of the sensor was 2.9% [29]. A cylinder-shaped sensor, which has been widely applied to electrochemical or metal oxide semiconductor sensors, was inherited to produce a CO_2 NDIR sensor. The dimensions of the cylinder were a 20-mm diameter and a 16.5-mm height. Parabolic mirrors were used to guide the light beam from an IR source to a detector. A glass bulb with a tungsten filament was used as the IR source of the sensor. A pyroelectric detector that covered a $4.26\text{-}\mu\text{m}$ BPF was used to measure the IR absorption of CO_2 . The sensor was reported to measure CO_2 from a few ppmv up to 20% with an accuracy of 1% [30]. Although these sensors could measure a large range of CO_2 , the relationship between the CO_2 level and the sensor signal (i.e., calibration curve) was not linear. This resulted in bias in the measurement of the middle range, because the sensor is generally calibrated at zero and span (i.e., 80–90% of the maximum measurement level). The linearity of the calibration curve is an important factor for the accuracy of an analyzer [33].

Thus, these sensors are suitable for detecting CO₂ or measuring the gas in cases that do not require a high accuracy of measurement results. For reliable inventory data that require high-quality research, an analyzer with a large measurement range and high accuracy in the full range (i.e., linear calibration curve) should be developed. Based on the Beer–Lambert law, the detection limit of a target gas using an NDIR analyzer depends on the IR absorbance of the target gas, the concentration of the target gas and the optical pathlength. Hence, to increase the lower detection limit of the analyzer, the concentration of the target gas and/or the optical pathlength should be increased. The concentrations of CO₂ are usually at the ppmv to percentage levels. Several experiments were carried out to evaluate the inlet concentration of target gases before introducing them into the analyzer [25,36,37]. Wang et al. (2010) used a pressure modulation to compress the inlet sample gas. The gas was compressed to 900 kPa. It was reported that the sensitivity of the measurement system was increased approximately 8.6 times [25]. An adsorbent was alternatively used to preconcentrate the inlet sample gas. Sklorz et al. (2010 and 2012) used Carbosieve S-II to accumulate ethylene before introducing it into an NDIR sensor. A 5 × 5-cm aluminum case was used to contain the Carbosieve S-II. The adsorption time was 1.6 min at 20 °C and 50 mL/min of flow rate. The desorption was conducted at 200 °C for 260 s. It was reported that the sensitivity was improved approximately 40 times [36,37]. The additional module, necessary to measure the accumulated concentration, leads to an increase in the cost of the analyzer and associated products. Therefore, the best way to improve the lower detection limit of the NDIR analyzer is to increase the optical pathlength. Optical White cells have been widely used to produce a multi-pathway gas cell for the NDIR analyzer. A White cell consists of three concave mirrors that have the same radius of curvature (see Figure 1) [38].

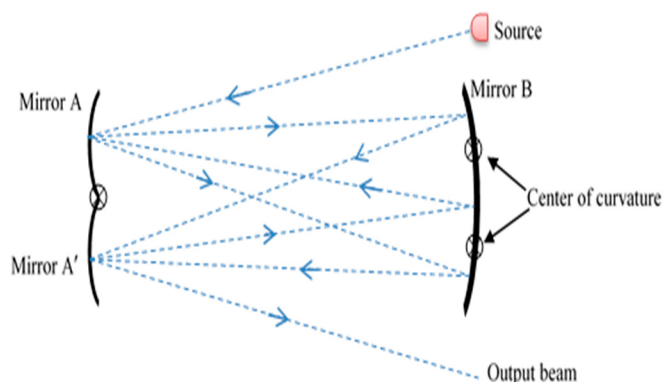


Figure 1. Diagram of the White cell principle.

The centers of mirrors A and A' are on the front surface of mirror B. The center of mirror B is at the halfway point between other two mirrors. The pathlength depends on the radius of curvature and the position of the centers of A and A' [38].

Consequently, this study was conducted to develop a wide-range CO₂ NDIR analyzer with high accuracy. To do that, practical pathlength ranges that were able to produce linear calibration curves from the ppmv to percentage levels were determined. Furthermore, the interference effects on the CO₂ NDIR analyzer were also investigated to help to improve the accuracy of the analyzer.

2. Experimental Methods

2.1. Investigation of the Effect of Pathlength on the Detection of CO₂

The NDIR analyzer consisted of a 20-W IR source (IR-Si253, Hawkeye Technologies Inc., Milford, CT, USA), a pyroelectric detector (LMM-335, Infratec GmbH, Dresden, Germany), a gas chamber with gold-coated mirrors and a waveguide coupled with a motor (0729, Bodine Electric Co., Northfield, IL, USA). The center wavelength of the IR BPF for CO₂ was 4.26 μm with a 180-nm half-bandwidth.

To reduce the drift of the analyzer, a reference BPF was applied. The center wavelength of the reference BPF was 3.95 μm with a 90-nm half-bandwidth. The experimental setup is presented in Figure 2.

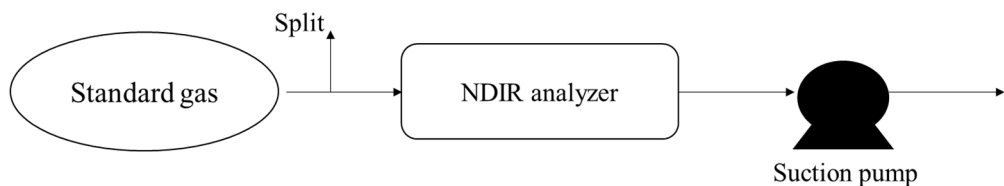


Figure 2. Experimental setup for a CO₂ nondispersive infrared (NDIR) analyzer.

In the gas chamber, the target gas absorbed IR light at its specific wavelength, resulting in a decrease of IR intensity at that wavelength. The IR intensity was measured by the detector and displayed as an electrical signal (called a detector signal). The logarithm of the ratio of the detector signal at reference BPF and the detector signal at CO₂ BPF was defined as the analyzer signal. The relationship between the target gas concentration and analyzer signal was evaluated.

The gas flow rate was 1 L/min, and the cell temperature was maintained at 45 °C to prevent condensation. The room conditions were 25 °C ± 1 °C and relative humidity (RH) = 40% ± 2%. The gas chamber volume was about 700 mL. Black anodized aluminum was used to make the gas chamber. The gas chamber size was 330 × 50 × 25 mm. The radius of the concave mirrors, based on White's principle, was 300 mm. The mirrors were gold-coated on glass substrate. The optical pathlengths of the gas cells were approximately 4.8-, 8-, 10.4- and 16-m.

First, N₂ (99.999%, DongA Ltd. Co., Gwangju, Republic of Korea) was used to calibrate the zero point. Then, CO₂ was used to calibrate the span points of the analyzer. The CO₂ concentration is shown in Table 1. After calibration, N₂ was introduced into the analyzer to determine the lower detection limit. The interval time for the recording was three minutes, and it was repeated 20 times [39]. The lower detection limit (*DL*) was calculated using the following Equation (1):

$$DL(\text{ppm}) = 2 \times \sqrt{\frac{\sum_{i=1}^{20} (C_i)^2 - \frac{1}{20} (\sum_{i=1}^{20} C_i)^2}{19}} \quad (1)$$

where C_i is the concentration displayed on the analyzer (ppm) at time i ($i = 0\sim20$) [39].

Table 1. Concentrations of target gases used in this study. BTEX: benzene, toluene, ethylbenzene and xylene.

Compound	Concentration (ppm, %-CO ₂)	Maker
CO	50, 150, 250, 350, 500	Rigas Co., Ltd., Daejeon, Republic of Korea
NO ₂	50, 150, 250, 350, 500	Rigas Co., Ltd., Daejeon, Republic of Korea
SO ₂	50, 150, 250, 350, 500	Rigas Co., Ltd., Daejeon, Republic of Korea
CO ₂	1.1, 2.3, 5.01, 7.4, 12.2, 17.3, 25	Rigas Co., Ltd., Daejeon, Republic of Korea
BTEX	20, 60, 100, 180	Rigas Co., Ltd., Daejeon, Republic of Korea
Formaldehyde	0.5, 1, 3, 5, 7, 9	Rigas Co., Ltd., Daejeon, Republic of Korea

The relative sensitivity can be practically defined as the slope of the calibration curve $y = f(x)$ between analyzer signals and concentrations of the target gas [40].

2.2. Investigation of the Interference Effects on the CO₂ NDIR Analyzer

On the basis of the results from Section 2.1, practical pathlengths for the ppmv level and the percentage level of the NDIR analyzer were selected. A general design of the flexible pathlength NDIR analyzer is presented in Figure 3. A short pathlength was used to measure the percentage level of CO₂,

which is defined as the percentage channel. A longer pathlength was used to measure the ppmv level of CO₂, which is called the ppmv channel. These channels were exchanged by varying the position of the movable mirrors (i.e., left/right-moving). The ppmv channel was used to measure CO₂ from 0 to 10,000 ppm. When the CO₂ concentration in the sample gas was over 10,000 ppmv, the percentage channel was used to measure CO₂. The maximum measurement level was 25%. The highest IR absorption gas in the indoor environment is H₂O. NO₂, SO₂ and CO also existed in the indoor air. They are also IR absorption gases [31,32]. Moreover, BTEX (i.e., benzene, toluene, ethylbenzene and xylene) and formaldehyde also showed significant amounts in the indoor air [41,42]. Consequently, the interference effects of these gases were investigated. The concentrations of these gases are shown in Table 1.

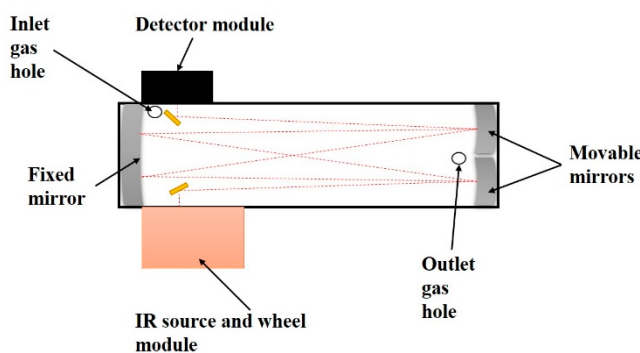


Figure 3. Schematic diagram of the wide-range NDIR with a flexible pathlength.

H₂O (vapor) was generated using the bubble method at 25 °C. On the basis of relative humidity, the humidity varied at 0%, 5%, 10%, 20%, 50% and 80%. Each concentration of each gas was introduced into the analyzer for 5 min. The experiment was repeated three times. The measurement error of the analyzer was tested using the Korean national standard method [39]. First, N₂ and CO₂ (20%) for the percentage channel and CO₂ (8000 ppmv) for the ppmv channel were used to calibrate the analyzer. Then, N₂ and CO₂ (10%) for the percentage channel and CO₂ (500 ppmv) for the ppmv channel were introduced into the analyzer to evaluate the accuracy. The experiment was repeated 5 times. To evaluate the continuous response of the analyzer, various concentrations of CO₂ were continuously introduced into the analyzer. A dilutor (Sonimix 2106-10, LNI Swissgas S.A., Versoix, Switzerland) was used to dilute 5.01% of CO₂ standard gas with N₂ to produce 4950 ppm and 1.02%, 1.51% and 5.01% of CO₂. Each level was introduced into the analyzer for 10 min.

The selectivity of the analyzer was used to determine the analytical accuracy. Selectivity presents the degree of free interference by other compounds in the sample [33]. The selectivity coefficient was calculated as Equation (2):

$$k_{B,A} = m_B/m_A \quad (2)$$

where A is the target analyte (i.e., NO gas in this study), B is the interfering compound, m_B is the slope of the calibration curve for compound B and m_A is the slope of the calibration curve for analyte A.

A comparison with other commercial devices was also carried out. For ppm levels of CO₂, the analyzer was compared with a CO₂ sensor (2211, Kanomax USA, Inc., Andover, NJ, USA). The measurement range of the sensor was 0 to 5000 ppmv. Its accuracy was ± 50 ppm. The comparison between the analyzer used in this study and the commercial sensor was conducted over 24 h. The CO₂ levels in our laboratory were measured. The laboratory conditions were 25 °C ± 2 °C and 40% ± 5% relative humidity. For percentage levels, the analyzer was compared with a CO₂ analyzer (60i; Thermo Fisher Scientific Inc., Franklin, MA, USA). The measurement range of the analyzer was 0% to 25% CO₂, with an accuracy of 0.05%. The comparison between the analyzer used in this study and the commercial analyzer was also conducted over 24 h. Since indoor CO₂ levels seldom reach percentage levels under normal conditions, except in fire events, the CO₂ emitted from an incinerator of biomass

was measured to compare. Due to the high moisture content in the flue gas, a moister pretreatment device was used to remove the moisture before introducing it into the analyzers. The humidity was maintained at less than 40% relative humidity at 25 °C. Due to differences in the time interval of each device, one-minute average data were used to compare them.

3. Results and Discussion

3.1. Investigation of the Effect of the Pathlength on the Detection of CO₂

The different beam patterns of the gas chamber are presented in Figure 4. In general, the pathway of the IR beam in the White cell depends on the angle of the mirror systems. Various angles resulted in different pathlengths of the NDIR gas cell. Besides, it was found that a gap between the two mirrors A and A' (as in Figure 1) also affected the pathlength. As a result, a practical equation to estimate the pathlength was found as follows:

$$L_o = 90 \times \sigma^{-1} \times R_f \times 10^{-3} \quad (3)$$

where L_o is the optical pathlength (m), σ is a gap between two movable concave mirrors (mm) and R_f is the radius of the concave mirror (mm).

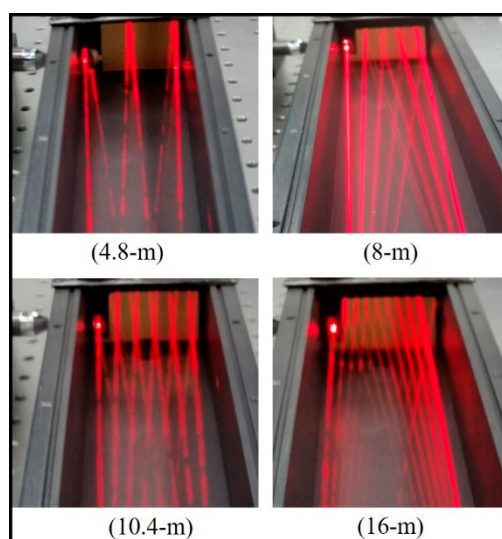


Figure 4. Patterns of different pathlengths in the NDIR gas chamber.

The relationships between the optical pathlength and the analyzer signals are depicted in Figure 5. Low values of standard deviation (SD) denoted good reproducibility of the experimental results. The sensitivity of the analyzer increased with the increase with the optical pathlengths. On the basis of the Beer–Lambert law, the increase of the pathlength resulted in an increase of the absorbance. Thus, this led to an improvement of the analyzer's sensitivity. However, since the IR absorbance of CO₂ was very strong, and its concentration was very high percentwise, most of its IR energy was absorbed. Therefore, the relationship between the analyzer signals and the CO₂ concentrations were nonlinear at long pathlengths (Figure 5b–d). In contrast, it was linear at the 4.8-m of pathlength (Figure 5a). As for CO₂ concentrations from 17% to 25%, sensitivities with respect to 4.8-, 8.0-, 10.4- and 16.0-m pathlengths were 0.045, 0.023, 0.006 and 0.002, respectively. Particularly, at 16.0 m of pathlength, the analyzer signals at 17% and 25% of CO₂ were 0.6282 and 0.6294, respectively. These analyzer signals reflected the IR absorption rate of CO₂, and they were almost similar. It suggests that the sensitivity at a high concentration of CO₂ should decrease with the increase in optical pathlength. Thus, longer pathlengths may not always translate into better results, in the case of high-IR absorption gases at high concentrations.

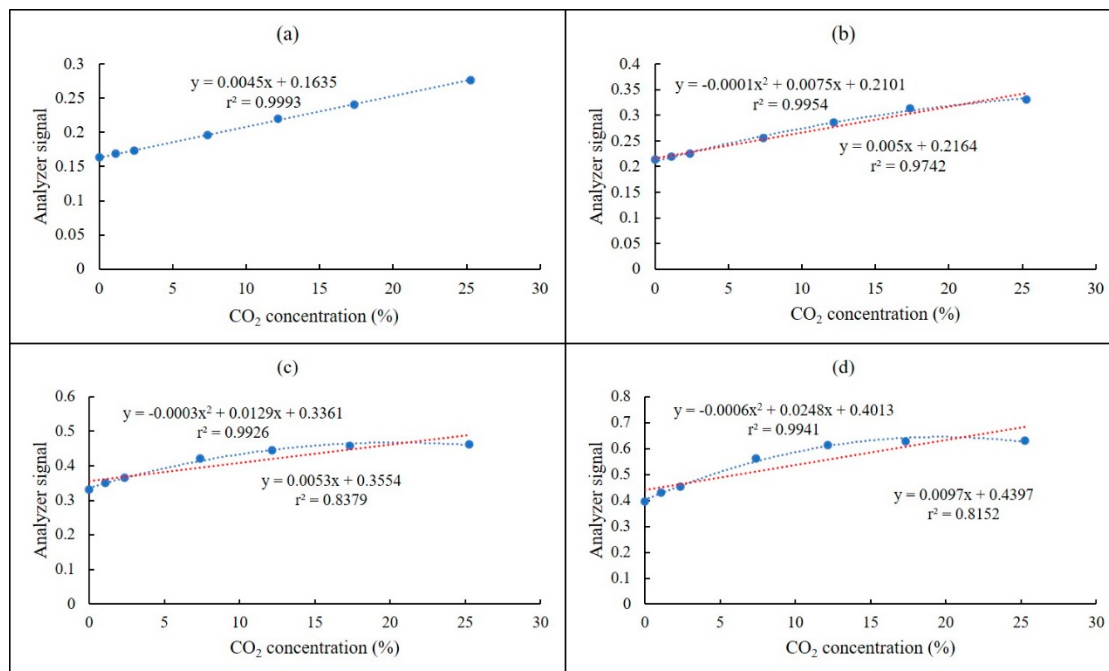


Figure 5. Variations of the analyzer signal associated with the pathlength and CO₂ concentration: (a) 4.8 m ($1.5 \times 10^{-5} < SD < 13.3 \times 10^{-5}$), (b) 8 m ($2.5 \times 10^{-5} < SD < 67.2 \times 10^{-5}$), (c) 10.4 m ($0.5 \times 10^{-5} < SD < 62.1 \times 10^{-5}$) and (d) 16 m ($0.5 \times 10^{-5} < SD < 35.2 \times 10^{-5}$).

Lower detection limits with respect to 4.8-, 8.0-, 10.4- and 16-m pathlengths are shown in Table 2. Thus, the 4.8-m pathlength could be used to measure the percentage level of CO₂ (i.e., 1% to 25%). The 10.4-m and 16-m pathlengths could be used to measure the ppmv level of CO₂ (i.e., 0 to 10,000 ppm). However, the lower detection limit at the 16-m pathlength did not show a significant difference to that at 10.4 m. Therefore, the 10.4-m pathlength was selected, in consideration of the cost and noise. Based on the Korean national standard method of NDIR analysis, the detection limit must be $\leq 1\%$ of the full scale. To meet this standard, the detection limit of the NDIR analyzer should be lower than 0.25% for CO₂, since the maximum measurement level of this analyzer was 25%. The lower detection limit of CO₂ was less than 0.25% at all tested pathlengths.

Table 2. Lower detection limits with respect to various pathlengths.

Pathlength (m)	Lower Detection Limit (ppmv)	Standard Deviation * (ppmv)
4.8	703	1.6
8.0	410	1.2
10.4	100	0.6
16.0	80	0.9

Note: * Standard deviation of 20 repetitions.

The lower detection limit decreased as the optical pathlength increased. This pattern matched the Beer–Lambert law. Other studies have shown similar results [29,30]. Hodgkinson et al. (2013) developed an NDIR sensor for CO₂ and reported that the pathlength of the NDIR sensor should be as long as possible in order to detect trace amounts of CO₂. An NDIR sensor for CO₂ has also been developed for breath analysis [29]. The pathlength of this NDIR sensor was varied, with pathlengths of 10, 20, 40 and 80 mm. That study demonstrated that an 80-mm pathlength detected CO₂ down to the ppm level, whereas high concentrations of CO₂ (up to 5%) could be detected by the 10-mm pathlength [29].

3.2. Effect of Interference Gases on the CO₂ NDIR Analyzer

From the above experimental results, we determined that the practical pathlengths for the CO₂ NDIR analyzer were 4.8 and 10.4 m. The optical pathlength of the percentage channel was 4.8 and that of the ppmv channel was 10.4 m. The calibration curves of CO₂ for the two channels are presented in Figure 6. Low values of standard deviation (SD) indicated that the analyzer had good reproducibility.

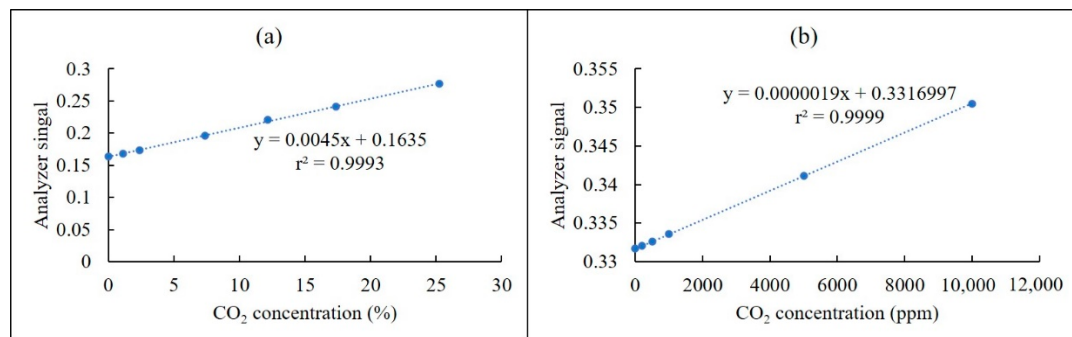


Figure 6. Calibration curves of the CO₂ NDIR analyzer at (a) the percentage channel ($1.5 \times 10^{-5} < SD < 13.3 \times 10^{-5}$) and (b) the ppmv channel ($1.5 \times 10^{-5} < SD < 5.0 \times 10^{-5}$).

The effects of CO, NO₂, SO₂, H₂O (vapor), BTEX and formaldehyde interference on the NDIR analyzer with respect to the percentage channel are depicted in Figure 7. Those with respect to the ppmv channel are presented in Figure 8. Linear regression curves and selectivity coefficients of those interference gases are shown in Table 3.

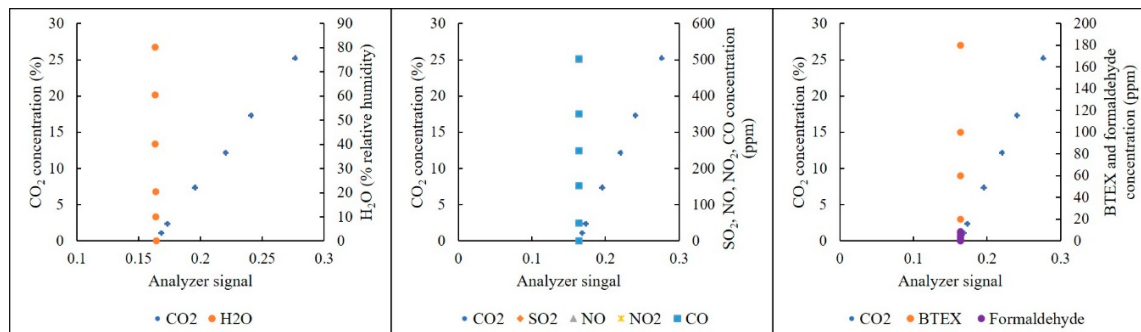


Figure 7. Effects of interference gases on the NDIR analyzer at the percentage channel.

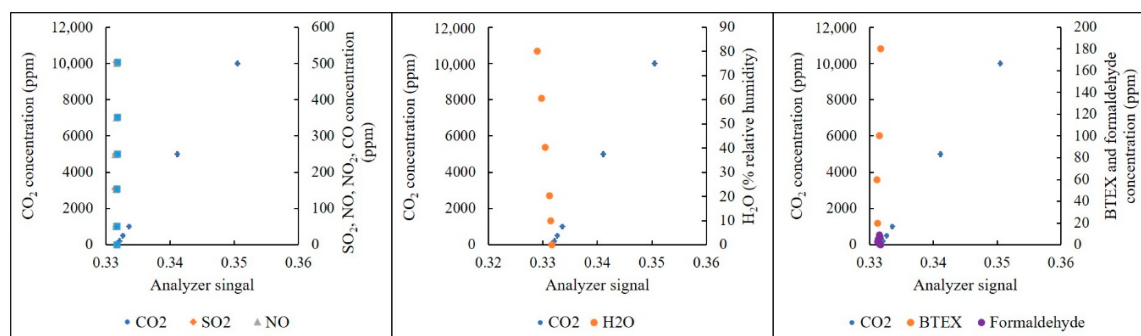


Figure 8. Effects of interference gases on the NDIR analyzer at the ppmv channel.

Table 3. Response of analyzer signal to interference gases with respect to percentage and ppmv channels.

Compound	Percentage Channel			ppmv Channel		
	Selectivity Coefficient	Linear Regression Curve	r^2	Selectivity Coefficient	Linear Regression Curve	r^2
SO ₂	2.22×10^{-5}	$Y = -1 \times 10^{-7}X + 0.1641$	0.0489	0.0842	$Y = 1.6 \times 10^{-7}X + 0.3316$	0.0484
NO	8.89×10^{-7}	$Y = 4 \times 10^{-9}X + 0.1640$	0.0002	0.0578	$Y = 1 \times 10^{-7}X + 0.3316$	0.0457
NO ₂	1.11×10^{-5}	$Y = -5 \times 10^{-8}X + 0.1640$	0.0036	0.0436	$Y = 8 \times 10^{-8}X + 0.3316$	0.0420
CO	2.44×10^{-5}	$Y = 1 \times 10^{-7}X + 0.1641$	0.9588	0.1526	$Y = 2.9 \times 10^{-7}X + 0.3317$	0.9853
BTEX	1.11×10^{-6}	$Y = -5 \times 10^{-9}X + 0.1641$	0.0001	0.6315	$Y = 1 \times 10^{-6}X + 0.3314$	0.1145
Formaldehyde	7.33×10^{-4}	$Y = 3 \times 10^{-6}X + 0.1640$	0.2067	0.6315	$Y = -1 \times 10^{-6}X + 0.3315$	0.0001
H ₂ O	2.44×10^{-3}	$Y = -1 \times 10^{-5}X + 0.1641$	0.9198	17.894	$Y = -3 \times 10^{-5}X + 0.3317$	0.9957

As shown in Figure 7 and Table 2, H₂O and CO revealed significant effects on the NDIR CO₂ analyzer ($r^2 > 0.90$) at the percentage channel. The selectivity coefficients of H₂O and CO were also higher than those of other gases. In general, since the CO concentration is at the ppm level in indoor air, the effect of CO can be neglected for the percentage level of CO₂. In contrast, the humidity is always high. Therefore, the effect of H₂O is significant. To compensate for this effect, a cross-interference factor can be used to improve the accuracy of the analyzer [28,43].

For the ppmv channel, H₂O and CO also displayed significant interference on the analyzer. In addition, the selectivity coefficients of all interference gases were also higher than those with respect to the 4.8-m pathlength. However, the concentrations of BTEX and formaldehyde in indoor air are usually at the ppb level [41]. Therefore, the effects of BTEX and formaldehyde on the analyzer were not significant. Since SO₂, NO and NO₂ are generally also at the ppb level, their effects are also negligible. In terms of CO interference, this gas should be taken into account, because the levels of CO₂ are also at the ppmv level. However, the interference was not very strong. Thus, the interference could be easily compensated by means of a cross-interference factor [28,43]. For H₂O, a moisture pretreatment device could be used to reduce the H₂O level. Then, the cross-interference factor could be applied [28,43]. For the cross-interference factors, a humidity sensor and a CO sensor were applied to measure the levels of the two gases. Then, the correlation factors of these gases to CO₂ were able to be calculated, and the errors caused by the two gases could be subtracted.

In terms of the measurement error, it was found that the measurement error of the CO₂ analyzer in this study was $\pm 0.4\%$ at the ppmv channel and $\pm 0.9\%$ at the percentage channel. The continuous response of the analyzer with regards to different levels of CO₂ is depicted in Figure 9. It was found that the measurement errors for continuous monitoring were also less than 0.4% and 0.9%, respectively, for the ppmv and percentage levels. Sun et al. (2013) reported that the measurement error of their prototype NDIR analyzer was $\pm 1\text{--}1.5\%$, and its detection limit of CO₂ (in the detection range of 0~17%) was $< 0.3\%$ [28]. Results of the comparison between the analyzer in this study and commercial products are presented in Figure 10. It was found that the relative percentage differences of the measurement data for 24 h between the analyzer used in this study and the commercial sensor/analyzer were 2.16% and 3.34%, respectively. Therefore, the CO₂ NDIR analyzer in this study was capable of the detection of CO₂ in indoor air at the ppmv, as well as the percentage, levels. At the ppmv level, the measurement results could be meaningfully applied for an indoor air quality assessment. At the percentage level, CO₂ might be used as an indicator for a fire alarm.

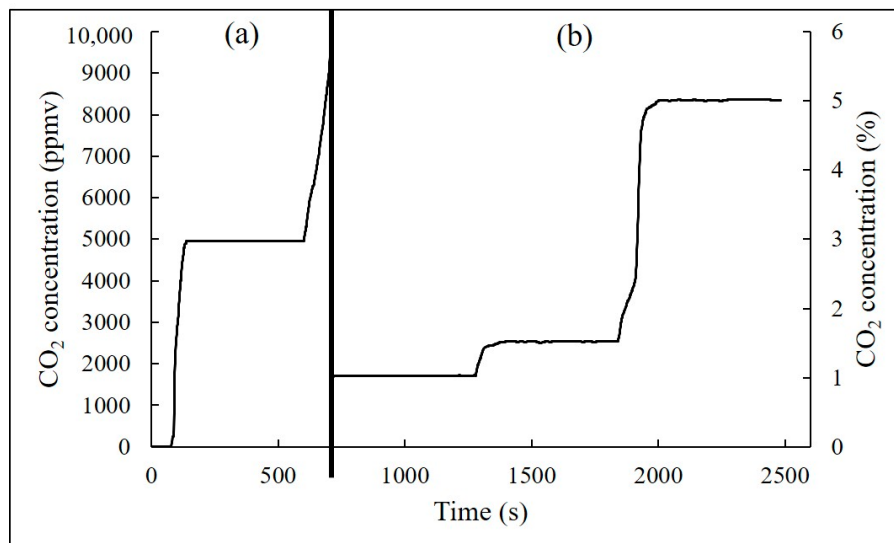


Figure 9. Variations of CO₂ concentrations observed from the analyzer with respect to various standard gas concentrations at the ppmv level (a) and at the percentage level (b).

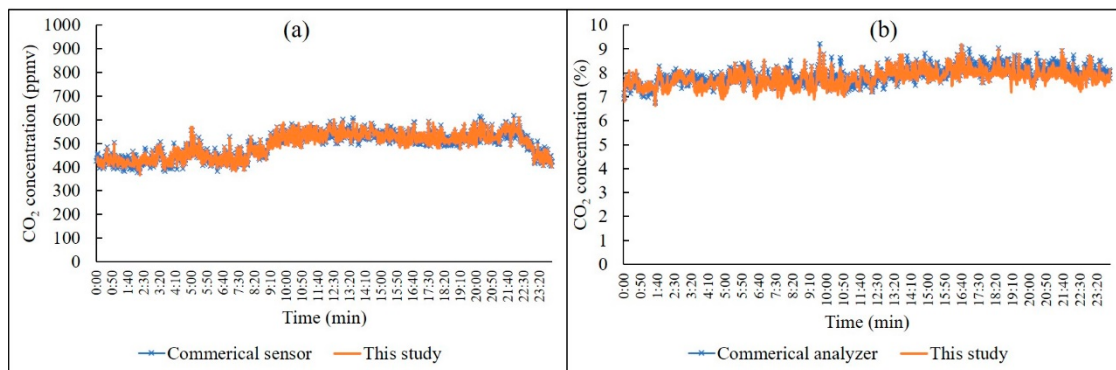


Figure 10. A comparison between the analyzer used in this study and a commercial device. Comparison at the ppmv level (a) and comparison at the percentage level (b).

4. Conclusions

A CO₂ NDIR analyzer for indoor air was developed in this study. Gold concave mirrors were used to produce the multi-pathway for the NDIR analyzer on the basis of an optical White cell. Experiments showed that the lower detection limit was inversely proportional to the pathlength and that the IR absorption intensity of the target gases depended on the intensity of the IR beam. It was found that the linear calibration curve could not be made regarding the wide range of CO₂ with the same pathlength. To produce linear curves, the pathlengths for the ppmv level and the percentage level should be separated. As a result, the practical range of the pathlength for CO₂ was 4.8 m to 10.4 m. Thus, a 4.8-m pathlength was applied for the measurement of the percentage level of CO₂, and a 10.4-m pathlength was done for the measurement of the ppmv level of CO₂. We also found that longer pathlengths did not always translate into better results for high-IR absorption gases at high concentrations. In terms of interference, CO, NO₂, SO₂, H₂O, BTEX and formaldehyde were investigated from 0 to high-ppm levels. It was found that H₂O caused significant interference on the CO₂ analyzer due to its high concentration in the indoor air. In contrast, CO only revealed a significant effect at the ppm levels. Therefore, the compensation for H₂O interference proved to be a pivotal issue for the development of a CO₂ analyzer using NDIR technology. The measurement errors were found to be 0.4% and 0.9% at the ppmv channel and the percentage channel, respectively. The maximum difference in the measurement data between the analyzer in this study and commercial instruments was found to be approximately

1.74%. This wide-range and high-accuracy CO₂ analyzer might help to improve the indoor air quality with better ventilation performance. The accurate measurement it provides might also be helpful for other studies on CO₂, such as indoor air quality assessments, indoor air quality metrics, ventilation control and building occupants' health, etc. In future studies, the long-term drift of the analyzer should be investigated to determine its recalibration duration. Since the analyzer proved to be relatively bulky for indoor applications, further works should be conducted to reduce the size of the analyzer.

Author Contributions: J.-C.K. and T.-V.D. conceptualized the work. T.-V.D. and J.-Y.L. performed the experiments. T.-V.D. wrote the original draft, and review and editing were done by J.-W.A. and J.-C.K. All authors have read and agreed to the published version of the manuscript.

Funding: This research was supported by the R&D Center for Green Patrol Technologies through the R&D for Global Top Environmental Technologies (Grant number—1485016147) funded by the Ministry of Environment (MOE), Republic of Korea.

Acknowledgments: This research was supported by the R&D Center for Green Patrol Technologies through the R&D for Global Top Environmental Technologies funded by the Ministry of Environment (MOE), Republic of Korea.

Conflicts of Interest: The authors declare no conflict of interest.

References

1. Hoefer, U.; Gutmachera, D. Fire Gas Detection. *Procedia Eng.* **2012**, *47*, 1446–1459. [[CrossRef](#)]
2. Gutmacher, D.; Hoefer, U.; Wöllensteiner, J. Gas sensor technologies for fire detection. *Sens. Actuators B Chem.* **2012**, *175*, 40–45. [[CrossRef](#)]
3. Fonollosa, J.; Solórzano, A.; Jiménez-Soto, J.; Moreno, S.O.; Marco, S. Gas Sensor Array for Reliable Fire Detection. *Procedia Eng.* **2016**, *168*, 444–447. [[CrossRef](#)]
4. Viveiros, F.; Gaspar, J.L.; Ferreira, T.; Silva, C. Hazardous indoor CO₂ concentrations in volcanic environments. *Environ. Pollut.* **2016**, *214*, 776–786. [[CrossRef](#)] [[PubMed](#)]
5. Chen, T.; Su, G.; Yuan, H. In situ gas filter correlation: Photoacoustic CO detection method for fire warning. *Sens. Actuators B Chem.* **2005**, *109*, 233–237. [[CrossRef](#)]
6. Jaber, A.R.; Dejan, M.; Marcella, U. The Effect of Indoor Temperature and CO₂ Levels on Cognitive Performance of Adult Females in a University Building in Saudi Arabia. *Energy Procedia* **2017**, *122*, 451–456. [[CrossRef](#)]
7. Shriram, S.; Ramamurthy, K.; Ramakrishnan, S. Effect of occupant-induced indoor CO₂ concentration and bioeffluents on human physiology using a spirometric test. *Build. Environ.* **2019**, *149*, 58–67. [[CrossRef](#)]
8. Du, C.; Wang, S.; Yu, M.; Chiu, T.; Wang, J.-Y.; Chuang, P.; Jou, R.; Chan, P.; Fang, C.-T. Effect of ventilation improvement during a tuberculosis outbreak in underventilated university buildings. *Indoor Air* **2020**, *30*, 422–432. [[CrossRef](#)]
9. Pereira, M.; Tribess, A.; Buonanno, G.; Stabile, L.; Scungio, M.; Baffo, I. Particle and Carbon Dioxide Concentration Levels in a Surgical Room Conditioned with a Window/Wall Air-Conditioning System. *Int. J. Environ. Res. Public Health* **2020**, *17*, 1180. [[CrossRef](#)]
10. Ramalho, O.; Wyart, G.; Mandin, C.; Blondeau, P.; Cabanes, P.-A.; Leclerc, N.; Mullot, J.-U.; Boulanger, G.; Redaelli, M. Association of carbon dioxide with indoor air pollutants and exceedance of health guideline values. *Build. Environ.* **2015**, *93*, 115–124. [[CrossRef](#)]
11. Zhou, J.; Kim, C.N. Numerical Investigation of Indoor CO₂ Concentration Distribution in an Apartment. *Indoor Built Environ.* **2010**, *20*, 91–100. [[CrossRef](#)]
12. Pamonpol, K.; Areerob, T.; Prueksakorn, K. Indoor Air Quality Improvement by Simple Ventilated Practice and *Sansevieria trifasciata*. *Atmosphere* **2020**, *11*, 271. [[CrossRef](#)]
13. American Society of Heating Refrigerating and Air Conditioning Engineers. *Ventilation for Acceptable Indoor Air Quality*; American Society of Heating Refrigerating and Air Conditioning Engineers: Atlanta, GA, USA, 2019.
14. Seppanen, O.A.; Fisk, W.J.; Mendell, M.J. Association of ventilation rates and CO₂ concentrations with health and other responses in commercial and institutional buildings. *Indoor Air* **1999**, *9*, 226–252. [[CrossRef](#)]

15. Pegas, P.N.; Alves, C.; Evtyugina, M.G.; Nunes, T.; Cerqueira, M.; Franchi, M.; Pio, C.; Almeida, S.M.; Freitas, M.C. Indoor air quality in elementary schools of Lisbon in spring. *Environ. Geochem. Health* **2010**, *33*, 455–468. [[CrossRef](#)]
16. Al-Rashidi, K.; Loveday, D.; Al-Mutawa, N. Impact of ventilation modes on carbon dioxide concentration levels in Kuwait classrooms. *Energy Build.* **2012**, *47*, 540–549. [[CrossRef](#)]
17. Yang, J.; Nam, I.; Yun, H.; Kim, J.; Oh, H.-J.; Lee, D.; Jeon, S.-M.; Yoo, S.-H.; Sohn, J.-R. Characteristics of indoor air quality at urban elementary schools in Seoul, Korea: Assessment of effect of surrounding environments. *Atmospheric Pollut. Res.* **2015**, *6*, 1113–1122. [[CrossRef](#)]
18. Shendell, D.G.; Prill, R.; Fisk, W.J.; Apte, M.G.; Blake, D.; Faulkner, D. Associations between classroom CO₂ concentrations and student attendance in Washington and Idaho. *Indoor Air* **2004**, *14*, 333–341. [[CrossRef](#)]
19. Morawska, L.; Tang, J.W.; Bahnfleth, W.; Bluyssen, P.M.; Boerstra, A.; Buonanno, G.; Cao, J.; Dancer, S.; Floto, A.; Franchimon, F.; et al. How can airborne transmission of COVID-19 indoors be minimised? *Environ. Int.* **2020**, *142*, 105832. [[CrossRef](#)]
20. Zellweger, C.; Emmenegger, L.; Firdaus, M.; Hatakka, J.; Heimann, M.; Kozlova, E.; Spain, T.G.; Steinbächer, M.; Van Der Schoot, M.V.; Buchmann, B. Assessment of recent advances in measurement techniques for atmospheric carbon dioxide and methane observations. *Atmos. Meas. Tech.* **2016**, *9*, 4737–4757. [[CrossRef](#)]
21. Institute of Clean Air Companies. *White Paper: Monitoring of HCl*; Institute of Clean Air Companies: Arlington, VA, USA, 2013.
22. Tarsa, P.B.; Lehmann, K.K. Cavity Ring-down biosensing. In *Optical Biosensors*; Elsevier BV: Amsterdam, The Netherlands, 2008; pp. 403–418.
23. Wang, J.; Tian, X.; Dong, Y.; Zhu, G.; Chen, J.; Tan, T.; Liu, K.; Chen, W.; Gao, X. Enhancing off-axis integrated cavity output spectroscopy (OA-ICOS) with radio frequency white noise for gas sensing. *Opt. Express* **2019**, *27*, 30517–30529. [[CrossRef](#)]
24. Chakraborty, N.; Mukherjee, I.; Santra, A.; Chowdhury, S.; Bhattacharya, S.; Mitra, A.; Sharma, C.; Chakraborty, S. Measurement of CO₂, CO, SO₂, and NO emissions from coal-based thermal power plants in India. *Atmos. Environ.* **2008**, *42*, 1073–1082. [[CrossRef](#)]
25. Wang, X.; Rödjemagård, H.; Oelmann, B.; Martin, H.; Larsson, B. High performance CO₂ measurement based on pressure modulation. *Procedia Eng.* **2010**, *5*, 1208–1211. [[CrossRef](#)]
26. Mayrwöger, J.; Reichl, W.; Hauer, P.; Krutzler, C.; Jakoby, B. CO₂ monitoring using a simple Fabry–Perot-based germanium bolometer. *Sens. Actuators B Chem.* **2011**, *154*, 245–250. [[CrossRef](#)]
27. Park, J.; Cho, H.; Yi, S. NDIR CO₂ gas sensor with improved temperature compensation. *Procedia Eng.* **2010**, *5*, 303–306. [[CrossRef](#)]
28. Sun, Y.; Liu, C.; Chan, K.L.; Xie, P.H.; Liu, W.Q.; Zeng, Y.; Wang, S.M.; Huang, S.H.; Chen, J.; Wang, Y.P.; et al. Stack emission monitoring using non-dispersive infrared spectroscopy with an optimized nonlinear absorption cross interference correction algorithm. *Atmos. Meas. Tech.* **2013**, *6*, 1993–2005. [[CrossRef](#)]
29. Vincent, T.; Gardner, J. A low cost MEMS based NDIR system for the monitoring of carbon dioxide in breath analysis at ppm levels. *Sens. Actuators B Chem.* **2016**, *236*, 954–964. [[CrossRef](#)]
30. Hodgkinson, J.; Smith, R.; Ho, W.O.; Saffell, J.R.; Tatam, R. Non-dispersive infra-red (NDIR) measurement of carbon dioxide at 4.2 μm in a compact and optically efficient sensor. *Sens. Actuators B Chem.* **2013**, *186*, 580–588. [[CrossRef](#)]
31. Stuart, B. Infrared Spectroscopy. In *Kirk-Othmer Encyclopedia of Chemical Technology*; Wiley: Hoboken, NJ, USA, 2005.
32. Wong, J.Y.; Anderson, R.L. *Non-Dispersive Infrared Gas Measurement*; Ifsa Publishing: Barcelona, Spain, 2012; ISBN 9788461597321.
33. Hanlan, J.; Skoog, D.A.; West, D.M. Principles of Instrumental Analysis. *Stud. Conserv.* **1973**, *18*, 45. [[CrossRef](#)]
34. Rogalski, A. *Infrared Detectors*, 2nd ed.; CRC Press Taylor & Francis Group: Oxfordshire, UK, 2011; ISBN 78-1-4200-7671-4.
35. Wright, J.; Lillesand, T.M.; Kiefer, R.W. Remote Sensing and Image Interpretation. *Geogr. J.* **1980**, *146*, 448. [[CrossRef](#)]
36. Sklorz, A.; Schafer, A.; Lang, W. Merging ethylene NDIR gas sensors with preconcentrator-devices for sensitivity enhancement. *Procedia Eng.* **2010**, *5*, 1192–1195. [[CrossRef](#)]
37. Sklorz, A.; Schafer, A.; Lang, W. Merging ethylene NDIR gas sensors with preconcentrator-devices for sensitivity enhancement. *Sens. Actuators B Chem.* **2012**, *170*, 21–27. [[CrossRef](#)]

38. White, J.U. Long Optical Paths of Large Aperture. *J. Opt. Soc. Am.* **1942**, *32*, 285. [[CrossRef](#)]
39. The Korea Ministry of Environment. *National Standard Method for Type Approval of Environmental Measurement Device (TM 0202.10)*; The Ministry of Environment: Sejong, Korea, 2017. Available online: <http://www.law.go.kr/admRulLsInfoP.do?admRulSeq=2100000185252#AJAX> (accessed on 22 September 2020).
40. Dijkstra, A.; Massart, D.L.; Kaufman, L. *Evaluation and Optimization of Laboratory Methods and Analytical Procedures*, 1st ed.; Elsevier Science: Amsterdam, The Netherlands, 1978; Volume 1, ISBN 9780080875484.
41. El-Hashemy, M.A.E.-S.A.; Ali, H.M. Characterization of BTEX group of VOCs and inhalation risks in indoor microenvironments at small enterprises. *Sci. Total. Environ.* **2018**, *645*, 974–983. [[CrossRef](#)] [[PubMed](#)]
42. Dai, X.; Liu, J.; Yin, Y.; Song, X.; Jia, S. Modeling and controlling indoor formaldehyde concentrations in apartments: On-site investigation in all climate zones of China. *Build. Environ.* **2018**, *127*, 98–106. [[CrossRef](#)]
43. Sun, Y.; Liu, W.-Q.; Zeng, Y.; Wang, S.-M.; Huang, S.-H.; Xie, P.; Yu, X.-M. Water Vapor Interference Correction in a Non Dispersive Infrared Multi-Gas Analyzer. *Chin. Phys. Lett.* **2011**, *28*, 073302. [[CrossRef](#)]



© 2020 by the authors. Licensee MDPI, Basel, Switzerland. This article is an open access article distributed under the terms and conditions of the Creative Commons Attribution (CC BY) license (<http://creativecommons.org/licenses/by/4.0/>).